2.2. SYNCHROTRON RADIATION

incident beam is diffracted by the sample and passes *via* a perfect analyser crystal [such as Si or Ge(111)] to the detector. The analyser crystal defines a very narrow angular acceptance for the diffracted radiation, determined by its Darwin width. The combination of the collimation of the incident radiation, its highly monochromatic nature and the stringent angular acceptance defines the instrument's excellent angular resolution. The detector arm supporting the analyser is scanned through the desired range of 2θ angles either in a step-scan mode or continuously, reading out at very short intervals the electronic modules that accumulate the detector counts.

To be transmitted by the analyser crystal, a photon must be incident on the crystal at the correct angle θ_a that satisfies the Bragg condition. The analyser crystal defines therefore a true direction (2θ angle) for the diffracted beam irrespective of where in the sample it originates from. This removes a number of aberrations that affect diffractometers with a scanning slit or PSD where the 2θ angle is inferred from the position of the slit or detecting pixel. Thus, with a capillary specimen, peak widths are independent of the capillary diameter, so a fat capillary of non-absorbing sample can be used to optimize diffracted intensity, and any modest misalignment of the sample from the diffractometer axis, or specimen transparency or surface roughness for flat-plate samples, does not lead to shifts in the peak positions. Modest movement of the sample with temperature changes in a furnace *etc.* does not cause shifts in peak positions. These instruments are therefore highly accurate, and are ideal for obtaining peak positions for indexing a diffraction pattern of a material of unknown unit cell (the first step in the solution of a structure from powder data), or following the evolution of lattice parameter with temperature *etc.* For flat samples, the $\theta/2\theta$ parafocusing condition does not need to be satisfied to have high resolution. The peak width does not therefore depend on sample orientation, which is useful for measurements of residual strain by the $\sin^2 \psi$ technique or for studying surfaces and surface layers by grazing-incidence diffraction. Interchange between capillary and flat-plate samples can easily be done as required without major realignment of the instrument. The stringent acceptance conditions also help to suppress parasitic scattering originating from sample-environment windows *etc.* and inelastic scattering such as fluorescence and Compton scattering.

On the other hand, at any 2θ angle only a tiny fraction of the diffracted photons can be transmitted by an analyser crystal, so this is a technique that consumes a lot of photons, and the high incident flux is essential to keep scan times to reasonable values. To overcome this, at least to some extent, Hodeau *et al.* (1998) devised a system of multiple analyser crystals, with nine channels mounted in parallel, each separated from the next by $2°$ (Fig. 2.2.10). In effect, as the detector arm is scanned, nine high-resolution powder-diffraction patterns are measured in parallel, each offset from the next by $2°$. If the data from the channels are to be combined, which is the usual procedure, the detectors must be calibrated with respect to each other, in terms of counting efficiency and exact angular offset, by comparing regions of the diffraction pattern scanned by several detectors (Wright *et al.*, 2003). A multianalyser system speeds up data collection significantly and can be found in various modified forms at a number of powder-diffraction beamlines (*e.g.* Lee, Shu *et al.*, 2008).

The multianalyser approach is best suited to capillary samples because of the axial symmetry of the arrangement. With flat plates in reflection, only one detector can be in the $\theta/2\theta$ condition where the effect of specimen absorption (for a sufficiently thick sample) is isotropic. Corrections must therefore be made to the
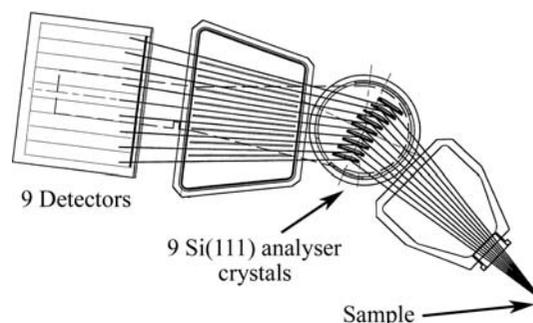
Figure 2.2.10
Multianalyser stage, nine channels separated by $2°$, devised by Hodeau *et al.* (1998), originally installed on the BM16 bending-magnet beamline at the ESRF with Ge(111) analyser crystals. With an undulator source, the greatly increased flux allows use of Si(111), which has a narrower Darwin width (by a factor of ∼2.4) and thus improved 2θ resolution, but with a lower fraction of the diffracted radiation accepted.

intensities from the other channels (Lipson, 1967; Koopmans & Rieck, 1968). For a capillary, choosing the wavelength and the diameter allows absorption to be kept to an acceptable value. Maximum diffracted intensity is expected at $\mu r = 1$ (where μ is the linear absorption coefficient and r the radius of the capillary), and below this value simple absorption corrections can be applied (Hewat, 1979; Sabine *et al.*, 1998). A value of μr greater than 1.5 begins to degrade the quality of the pattern significantly. If a sample with high absorption is unavoidable, such as when working close to an absorption edge of an element, *e.g.* the K edge of Mn at 6.539 keV (1.896 Å), then it can be preferable to stick a thin layer of sample on the outside of a 1-mm-diameter capillary. The shell-like nature of the sample has no effect on the peak shape or resolution because of the use of analyser crystals.

Capillaries also have the advantage that preferred orientation can be significantly less as compared to a flat sample, where there is a tendency for crystallites to align in the surface layers, especially if compressed to hold the powder in place. Spinning or otherwise moving the sample is necessary, whether capillary or flat plate, to increase the number of crystallites appropriately oriented to fulfil the Bragg condition and avoid a spotty diffraction pattern, the likelihood of which is exacerbated by the highly collimated nature of the incident radiation.

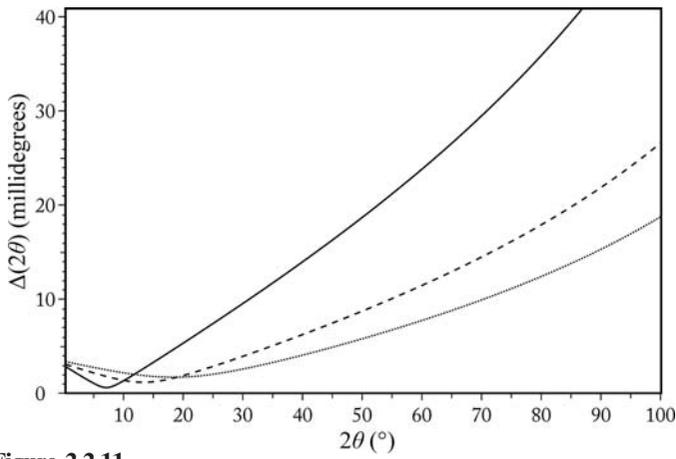### 2.2.4.1.1. *Angular resolution*

Various authors (*e.g.* Sabine, 1987*a*,*b*; Wroblewski, 1991; Masson *et al.*, 2003; Gozzo *et al.*, 2006) have discussed the resolution of a synchrotron-based diffractometer equipped with a double-crystal monochromator and an analyser crystal. The most usual setting of the diffracting crystals, ignoring any mirrors or other optical devices, is non-dispersive, alternatively described as parallel or $(1, -1, 1, -1)$.

The approach developed by Sabine (1987*a*,*b*) involves modelling the vertical divergence of the source and the angular acceptance of the monochromator and analyser crystals as Gaussian distributions with the same full width at half-maximum (FWHM) as the real distributions, and considering a powder as a crystal with an infinite mosaic spread. The rocking curve of the analyser crystal (equivalent to rocking 2θ) is given by

$$I(\beta) = \int \int d\alpha \, d\delta \exp\left\{-\left[\left(\frac{\alpha}{\alpha'_m}\right)^2 + 2\left(\frac{\delta - \alpha}{\Delta'_m}\right)^2 + \left(\frac{b\delta + \alpha - \beta}{\Delta'_a}\right)^2\right]\right\},$$

where

Figure 2.2.11

$\Delta(2\theta)$ calculated from equation (2.2.2) for a beamline with a double-crystal Si(111) monochromator, an Si(111) analyser ($\Delta_m = \Delta_a$ and $\theta_m = \theta_a$) and an FWHM vertical divergence of 25 µrad at $\lambda = 0.4$ Å (solid line: $\Delta_m \simeq 8.3$ µrad, $\theta_m = 3.6571°$), $\lambda = 0.8$ Å (dashed line: $\Delta_m \simeq 16.6$ µrad, $\theta_m = 7.3292°$) and $\lambda = 1.2$ Å (dotted line: $\Delta_m \simeq 25.2$ µrad, $\theta_m = 11.0319°$).

$$b = \tan\theta_a/\tan\theta_m - 2\tan\theta/\tan\theta_m.$$

Here α represents the vertical divergence from the source, δ is the difference between the Bragg angles of a central ray reflected from the monochromator at the angle θ_m and of another ray at angle θ'_m such that $\delta = \theta'_m - \theta_m$, and θ_a is the Bragg angle of the analyser crystal. The terms α'_m, Δ'_m and Δ'_a are related to the FWHM of the Gaussians representing the vertical divergence distribution or the Darwin widths of the monochromator and analyser crystals, α_m, Δ_m and Δ_a, respectively, with

$$\alpha'_m = \alpha_m/2(\ln 2)^{1/2}, \quad \Delta'_m = \Delta_m/2(\ln 2)^{1/2}, \quad \Delta'_a = \Delta_a/2(\ln 2)^{1/2}.$$

From the above equation, the intrinsic FWHM of the Gaussian-approximated peaks of the powder-diffraction pattern can be obtained as

$$\Delta^2(2\theta) = \alpha_m^2\left(\frac{\tan\theta_a}{\tan\theta_m} - 2\frac{\tan\theta}{\tan\theta_m} + 1\right)^2 + \tfrac{1}{2}\Delta_m^2\left(\frac{\tan\theta_a}{\tan\theta_m} - 2\frac{\tan\theta}{\tan\theta_m}\right)$$
$$+ \Delta_a^2. \tag{2.2.2}$$

Note that the true peak shape is not Gaussian, and a pseudo-Voigt (*e.g.* as described by Thompson *et al.*, 1987), Voigt (*e.g.* Langford, 1978; David & Matthewman, 1985; Balzar & Ledbetter, 1993) or other function modelled from first principles (*e.g.* Cheary & Coelho, 1992; Ida *et al.*, 2001, 2003) is usually better. Examples of FWHM curves calculated from equation (2.2.2) are plotted in Fig. 2.2.11 at three wavelengths. Differentiating the Bragg equation gives $\Delta d/d = -\cot\theta\,\Delta(\theta)$, where θ is in radians.

Gozzo *et al.* (2006) have extended the formulation of Sabine to include the effects of collimating and focusing mirrors in the overall scheme. Axial (horizontal) divergence of the beam between the sample and the detector causes shifts and broadening of the peaks, as well as the well known low-angle peak asymmetry due to the curvature of the Debye–Scherrer cones. Sabine (1987b), based on the work of Hewat (1975) and Hastings *et al.* (1984), suggests the magnitude of the broadening, $B(2\theta)$, due to horizontal divergence Φ can be estimated *via*

$$B(2\theta) = (\tfrac{1}{4}\Phi)^2(\cot 2\theta + \tan\theta_a),$$

where B and Φ are in radians. This value is added to $\Delta(2\theta)$.

2.2.4.1.2. *Hart–Parrish design*

A variant of the parallel-beam scheme replaces the analyser crystal with a set of long, fine Soller collimators (Parrish *et al.*, 1986; Parrish & Hart, 1987; Parrish, 1988; Cernik *et al.*, 1990; Collins *et al.*, 1992) (Fig. 2.2.12). The collimators define a true angle of diffraction, but with lower 2θ resolution than an analyser crystal because their acceptance angle is necessarily much larger and so the transmitted intensity is greater. They are not particularly suitable for fine capillary specimens, as the separation between foils may be similar to the capillary diameter, resulting in problems of shadowing of the diffracted beam. However, they are achromatic, and so do not need to be reoriented at each change of wavelength, which may have advantages when performing anomalous-scattering studies around an element's absorption edge. Unlike an analyser crystal, however, they do not suppress fluorescence. Peak shapes and resolution can be influenced by reflection of X-rays from the surface of the foils, or any imperfections in their manufacture, *e.g.* if the blades are not straight and flat. The theoretical resolution curve of such an instrument can be obtained from equation (2.2.2) by setting $\tan\theta_a$ to zero and replacing the angular acceptance of the analyser crystal Δ_a with the angular acceptance of the collimator Δ_c.

2.2.4.2. *Debye–Scherrer instruments*

The simplest diffractometer has a receiving slit at a convenient distance from the sample in front of a point detector such as a scintillation counter. The height of the slit should match the capillary diameter, or incident beam height for flat plates. A slightly larger antiscatter slit near the sample should also be employed to reduce
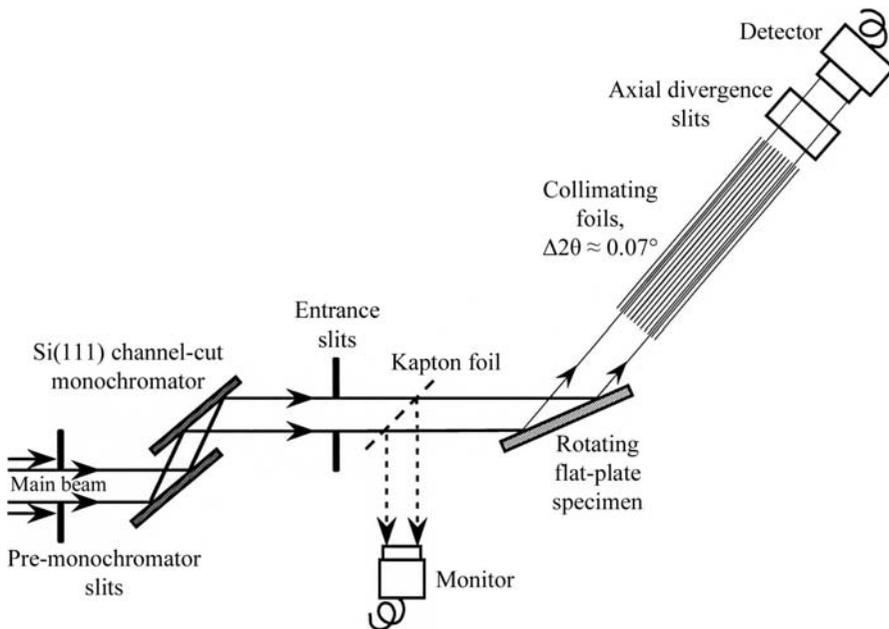
Figure 2.2.12

Schematic representation of a parallel-beam diffractometer of the Hart–Parrish design. The collimators installed on Stations 8.3 and 2.3 at the SRS Daresbury (Cernik *et al.*, 1990; Collins *et al.*, 1992) had steel blades 50 µm thick, 355 mm long, separated by 0.2 mm spacers, defining a theoretical opening angle (FWHM Δ_c) of 0.032° and a transmission of 80%.

references